Using a Genetic Algorithm to Update Convolutional Neural Networks for Abnormality Classification in Mammography

Steven Wessels and Dustin van der Haar[a]
Academy of Computer Science and Software Engineering, University of Johannesburg, Kingsway Avenue and University Road, Auckland Park, South Africa

Keywords: Computational Optimisation, Deep Learning, Computer Vision, Mammography.

Abstract: The processing of medical imaging studies is a costly and error-prone task. The use of deep learning algorithms for the automated classification of abnormalities can aid radiologists in interpreting medical images. This paper presents a genetic algorithm that is used to fine-tune the internal parameters of convolutional neural networks trained for abnormality classification in mammographic imaging. We used our genetic algorithm to search for the neural network weights representing the global minimum solution for ResNet50 and Xception architectures. The Xception architecture outperformed the ResNet baseline for both tasks, with the Xception baseline model achieving an AUC score of 72%. The genetic algorithm demonstrated a slight proclivity for improving the general metric evaluations of the network that it fine-tuned, but in some cases, it was still prone to miss good regions in the search space.

1 INTRODUCTION

The number of medical imaging studies is increasing disproportionately to the number of professional radiologists required to perform interpretation and diagnosis. As a result, the timely analysis of medical images becomes a bottleneck in the healthcare workflow. The increasing pressure placed on radiologists and the error and subjectivity inherent when interpreting medical images results in many misdiagnoses. To address the aforementioned issues, computer-aided detection and diagnosis systems have been proposed to aid clinicians. However, the early iteration of such systems, which used manual and task-specific feature extraction techniques, have yet to match the sensitivity of professional radiologists consistently and tend to generate many false-positive classifications. Deep learning methodologies have resulted in state-of-the-art performance on common computer vision tasks and demonstrated efficacy for performing radiological imaging analysis.

In this paper, we investigate the optimisation of deep learning methodologies for performing the task of abnormality classification in mammographic imaging. We also propose using a genetic algorithm to fine-tune our solutions without needing external contexts, such as the neural network's gradient information or knowledge of internal neuron connectivity. We present the experiment and results of a genetic algorithm that used a shared neural network representation to fine-tune the model trained using gradient descent and backpropagation. The abnormality classification task was performed independently using ResNet50 and Xception architectures.

The remainder of this study is structured in the following manner: Section 2 provides a brief description of the issues within the domain of mammography and radiology concerning image analysis. In section 3, we discuss similar work that attempts to use convolutional neural networks (CNN) to classify mammogram abnormalities. Section 4 presents the concept of computation optimisation and outlines the implementation details of the genetic algorithm used in this paper. In Section 5, we detail the data used to evaluate our model and outline the experimental configurations used to generate the results. Experimental validation results are discussed in section 6.

2 PROBLEM BACKGROUND

Aspects of medicine, such as disease diagnosis and treatment, have been revolutionised through the use of X-rays for ionising radiation to produce medical images (Dauer, 2019). Furthermore, the quality of healthcare has been greatly improved through diagnostic radiology. In oncology, radiology is central

---

[a] https://orcid.org/0000-0002-5632-1220

Wessels, S. and van der Haar, D.
Using a Genetic Algorithm to Update Convolutional Neural Networks for Abnormality Classification in Mammography.
DOI: 10.5220/0011648500003411
In *Proceedings of the 12th International Conference on Pattern Recognition Applications and Methods (ICPRAM 2023)*, pages 790-797
ISBN: 978-989-758-626-2; ISSN: 2184-4313

to the detection, staging, and management of cancer (Crean et al., 2012). Mammography uses X-ray imaging to examine the human breast for diagnosis and screening. The aim of examining mammographic images is to identify characteristic masses or microcalcifications that are indicative of breast cancer. Cancer screening has been shown to have helped reduce breast cancer mortality by 30% according to a three-decade-long study by Swedish doctors (Tabár et al., 2011).

Traditionally, mammograms would have to be inspected by a radiologist for signs of breast cancer. Manual inspection is an error-prone, costly, and time exhausting task. To alleviate the challenges associated with manual inspection, computer-aided detection and diagnosis systems that used pattern recognition and learning algorithms for inspection were designed and deployed (Kooi et al., 2017). By 2008, a reported 74% of all mammography examinations were screened using computer-aided diagnosis (CAD) (Kim et al., 2018). Following deep learning's rise to prominence following the state-of-the-art results achieved on the ImageNet data set, it was not long before researchers began investigating the efficacy of CNNs in a wider range of applications, including within the field of radiology. We will present these efforts in section 3. What will be apparent is that there are still many challenges preventing a workable and reliable solution from being found. The gradient-based methods ubiquitous for training neural networks have issues overcoming local minima and often converge slowly. Meta-heuristic algorithms, such as the evolutionary algorithm, are inspired by naturally occurring phenomena and are often efficient solutions to finding global optima in complex search spaces (Noel, 2012).

3 SIMILAR WORK

In 2019, Tsochatzidis et al. performed a comparative study of major CNN architectures regarding the classification of abnormalities found in the CBIS-DDSM, comparing the end-to-end performance of various deep learning architectures (Tsochatzidis et al., 2019). Their research aimed to compare the use of pretrained weights to the random initialisation of network parameters. The architectures compared were:

1. Alexnet: A relatively shallow network with five convolutional layers and three fully connected layers, regularised with dropout = 0.5.
2. VggNets: Both 16 and 19-layer variations were part of the comparative study.
3. ResNets: The variations 50, 101, and 152 were compared here.
4. GoogLeNet: The state-of-the-art V3 network was used.

In addition to using the CBIS-DDSM, the DDSM-400, another subset of the DDSM, was used for comparisons on abnormality classification. From the CBIS-DDSM, only cases containing masses were used. The images were preprocessed by cropping a window of 1024×1024 pixels centred around the mass for all lesions on the basis that this would avoid resize-induced distortion while including necessary adjacent tissue for learning features in larger scales. All input image sizes were set to 224×224 pixels. Additionally, data augmentation was used to create supplementary artificial samples of the data set by applying rotational and reflectional transformations to existing images. The authors argue that performing augmentation with the aforementioned transformations generates meaningful examples whereby rotation invariance for the learned features is implied. The from-scratch experiments used Glorot/Xavier initialisation, while the pre-trained networks had their convolutional layers initialised with Imagenet weights, and their final layers were randomly initialised. The Adam optimiser was used to train all networks. For every architecture they compared, the pre-trained achieved a higher area under the curve (AUC) and accuracy scores in fewer epochs than their end-to-end counterparts, proving the efficacy of using pre-trained networks over training models end-to-end. The pre-trained ResNets achieve the best metric results, with ResNet50 outperforming their deeper counterparts with an AUC of 80.4%. Interestingly, the ResNets outperformed when trained from scratch compared to the VggNets and AlexNet. The authors suggested that the complexity and depth of ResNets are the cause of this discussion point.

Recently, Almeida et al. also performed a comparative study on the CBIS-DDSM for abnormality classification (Almeida et al., 2021). They compared XGBoost, a gradient-boosted trees algorithm, to VGGNet16 using three different data set configurations, including a full data set configuration relevant to our study. The authors also used data augmentation to supplement the data set by applying random horizontal reflections, rotation about the origin, shear transformation, vertical and horizontal shifts, and cropping in. An image input size of 224×224 pixels was used. Similar to Tsochatzidis et al., the authors of (Almeida et al., 2021) compared a network with pre-trained Imagenet weights to a from-scratch variant. Their best-performing VGGNet model was the pre-trained variant which achieved an AUC of 68.22%.

With regards to literature specifically pertaining to training CNNs using meta-heuristic algorithms, Pawełczyk et al. used a genetic algorithm in combination with the backpropagation algorithm to update the weights of a LeNet-4 CNN architecture (Pawełczyk et al., 2018). Their population was comprised of individuals representing the weights that encoded the CNN, with the initial weight values being drawn from a uniform distribution. The fitness of solutions was calculated using classification error. A combination of elitist and random selection was used to draw a new population for recombination. The crossover was performed at a single point per layer. They validated their model against the MNIST data set and found that their GA-Backpropagation method outperformed the classical gradient-based back-propagation optimisation method.

4 METHODS

4.1 Computational Intelligence for Optimization Problems

Computational intelligence is a sub-field of artificial intelligence that enables intelligent behaviour within complex search spaces. Meta-heuristic algorithms are versatile and adaptable problem-solving programs utilised on computational optimisation problems for which no efficient problem-specific algorithm exists. In this section, we present a population-based stochastic search paradigm from the field of computational intelligence that can be used for optimisation tasks.

Evolutionary computing uses models based on biological evolution to solve optimisation processes (Engelbrecht, 2008). The overarching idea of evolutionary computing is that the simulated evolutionary process improves solutions generated by an evolutionary computation system through exposure to dynamic and competitive environments. Genetic algorithms were the earliest and most fundamental method of simulation evolution with computing systems. John Holland is considered the chief proponent of genetic algorithms in optimisation due to his extensive work in the field and his proposition of the canonical genetic algorithm (Holland, 2010). A generic genetic algorithm will follow the following iterative process: 1) Evaluation of each individual's fitness 3) Reproducing to produce offspring 4) Selection of the next generation.

The fundamental constituent variables of evolutionary algorithms are chromosomes, where the data encoded into the chromosome defines the representation of a solution. These characteristics, also known as genes, hold data values relevant to forming a solution. A population of chromosomes compete to reproduce offspring based on the strength of an individual's solution. A fitness function is used to measure a solution's objective value based on the constraints of a given problem. The crossover process is where parts of two reproducing solutions are used to form new solutions. A small number of genes in the new solution can be randomly changed or mutated, creating evolution within the population of solutions. Only the fittest chromosomes are likely to be moved to the next generation between the newly generated solutions and the existing population.

Selection algorithms are a mechanism used to determine which individuals in a population get to reproduce based on their fitness. Selection is the driving force behind achieving a better solution (Engelbrecht, 2008). Random selection is the simplest of all selection algorithms. Each individual has the same probability of being chosen to continue to the next generation, regardless of their fitness. Theoretically, randomly selecting members from the population to continue and reproduce should result in the longest takeover time, i.e. the time taken to achieve convergence. Random selection will be the baseline for the comparison. Roulette selection gives an individual a chance of being selected that is directly proportional to their fitness value relative to other individuals in the population. This selection mechanism may limit the diversity of solutions. Rank selection orders the population concerning their fitness values. The highest-ranking member is the fittest individual, and the lowest-ranked member is the worst of the generation. The advantage of rank selection over roulette selection is that the best-performing individuals don't skew the selection process by such a large degree. Tournament selection randomly chooses a subset of the population to compete against one another, with the best-performing individual chosen to continue to the next generation. The size of the tournament set ought to be carefully chosen. A large tournament set size results in the fittest individuals dominating, while a small size increases the number of unfit individuals in the next generation (Miller and Goldberg, 1995). Elitism is used to ensure the survival of the best individual of a population and is not necessarily a means of selecting all the individuals who will go on to the next generation, as with other selection schemes.

Using meta-heuristic algorithms to search for parameters to minimise a network's loss function can be comparable to evolving a linked set of connected weights. One of the main benefits meta-heuristics provide over gradient descent methods is that they require no context information about the space they search, apart from the objective function (Whitley et al., 1990). Critically, no gradient information is required. In the case of genetic algorithms, selective reproduction and recombination of encoded solutions change the sampling rate of hyperplanes in the search space to indicate the average fitness of solutions that belong in any particular hyperplane. This sampling rate change removes the need to search along the contours of the objective function, which in turn mitigates the likelihood of the search becoming stuck in local minima. A challenge the GA will face is optimising large numbers of weights present in convolutional neural networks since neither search technique is known to scale well (Whitley et al., 1990) (Oldewage, 2017). A general cause of scale issues for meta-heuristics is the sheer number of existing solutions, which increases the difficulty of ascertaining whether or not certain regions in the search space represent “good” regions.

The gradient-based methods ubiquitous for training neural networks have issues overcoming local minima and often converge slowly. Meta-heuristic algorithms, such as the genetic algorithm (GA), are inspired by naturally occurring phenomena and are often efficient solutions to finding global optima in complex search spaces (Noel, 2012). We will therefore investigate the use of meta-heuristic algorithms to refine the parameter optimisation with a predisposition for lowering false positive rates.

We use a genetic algorithm for parameter learning to compare meta-heuristic methods. The individuals of a population are represented by a vector of length *N*, where *N* is the number of layers of trainable weights in the CNN. Within each element of this vector is another vector containing the layer’s weights. Representing the solution using the same logical structure as the CNN’s weights vector is the most programmatically simple method of encoding our chromosomes. This representation scheme allows us to maintain operational context by preventing modification to the logical structure of a network’s internal parameters. We also preserve the spatial relationship caused by CNN’s translation invariance property. However, our solution encoding imposed serious constraints on the model’s training. The size of the population used for the algorithm and the number of generations that the algorithm can run for will be minimal because of the extra memory requirements of having to keep “copies” of the weight vectors during training and the computational requirements to calculate the loss for each solution.

To initialise the population, we first create a particle using the current weights of the model and then generate the remaining particles by multiplying each weight by a randomly sampled float in the range $(0,1)$. We then find the fittest solution in the population using the objective function before starting the first iteration. The objective function used will depend on the machine learning task being performed. For classification tasks, the objective function used to evaluate the validity of a solution when provided with predicted values $\mathbf{\acute{y}}$ and corresponding ground truth labels $\mathbf{y}$ is the following:

Algorithm 1: Genetic algorithm to update network parameters.

```
Require: Generations $n$
Require: Crossover threshold $C_t$
Require: Population size $P$
Require: Tournament size $T$
Require: Culling size $K$
Require: Fitness function $f$
Require: The trainable parameters $\theta$
  Initialize solution population
  while $n \leq n_{max}$ do
    Evaluate fitness of all solutions $f(\theta)$
    while Next generation population size ¡ Current population size do
      Remove $K$ weakest individuals from population
      Perform tournament selection to select $\theta_1$ and $\theta_2$
      where $f(\theta_1) < \theta_2$
      if Chance of reproduction$> C$ then
        Perform 2-point crossover with $\theta_1$ and $\theta_2$ to create new solution $\theta'$
        Add $\theta'$ to next generation
      else
        Mutate $\theta_1$ and add to next generation
      end if
      Advance to the next generation, $n = n + 1$
    end while
  end while
```

$$\begin{aligned} f(\mathbf{\acute{y}},\mathbf{y}) &= 2 \times loss(\mathbf{\acute{y}},\mathbf{y}) + FPR(\mathbf{\acute{y}},\mathbf{y}) \\ &+(1-TNR(\mathbf{\acute{y}},\mathbf{y})) + (1-ACC(\mathbf{\acute{y}},\mathbf{y})) \end{aligned} \tag{1}$$

where FPR is the function that calculates the false positive rate and TNR calculates the specificity. The loss function used was binary cross entropy. Using this objective function, we can explicitly predispose the algorithm to minimise false positive cases by considering the false positive rate and the inverse true negative rate to address a common shortcoming of CAD systems.

Following the initial population creation and fitness calculation, the next generation of solutions must be selected. We use an elitist scheme to ensure that the best individuals of a previous generation survive to the next generation. Elitism is a highly exploitative technique that can cause the algorithm to favour a local minimum instead of exploring the search space. However, since the GA is being used to refine the search initiated by a gradient descent algorithm, we feel that the exploitation of a search space is appropriate. Our elitist scheme guaranteed that the top three fittest individuals would continue to the next generation. We then use tournament selection to choose the individuals to perform crossover to produce the remaining members of the next generation. Tournament selection randomly chooses a subset of the population to compete against one another. The two best-performing individuals are selected to perform crossover to produce a new individual for the next generation. The size of the tournament subset ought to be carefully chosen, as a large tournament subset size results in the fittest individuals dominating, while a small size increases the number of unfit individuals in the next generation (Engelbrecht, 2008). The tournament selection algorithm used in the model presented used 12% of the population for a tournament set size, a size we found through experimentation to be beneficial to minimise the performance overhead and balance the passing of strong genetic material while still allowing for exploration. Once tournament selection determines the two best individuals from the tournament subset, a random number between 0 and 100 is produced to determine if a crossover will occur with the selected individuals to produce a new solution. If the crossover threshold is met, an elementwise crossover algorithm generates a new solution with the genetic material chosen by a coin toss. The mutation is also applied elementwise with a 0.5% chance of an element being mutated by multiplication of a range of $(-1,1)$. If the crossover threshold is not met, then the winner of the tournament selection is added to the next generation. After the GA has run for ten generations, the best individual weights are fitted to the CNN model for evaluation.

4.2 Convolutional Neural Networks

We used two convolutional neural network architectures to evaluate the genetic algorithm's parameter fine-tuning ability. It is the smallest variant of the ResNet family of networks and gives us the fewest number of parameters to train. Despite having low network depth relative to other ResNets, ResNet50 attained very high-performance metrics on the ImageNet data set, with a top-1 accuracy of 0.749 and a top-5 accuracy of 0.921 (Keras, 2017). We would also investigate the classification performance of Xception, a modern network with fewer weights than ResNet50 and slightly better scores on ImageNet, with top-1 accuracy of 0.790 and top-5 accuracy of 0.945.

4.3 ResNet50

The name ResNet50 is derived from the fact that the network is comprised of fifty weighted layers and four residual blocks. The total number of trainable parameters contained in ResNet50 is 24577026. The input is fed into a convolutional layer where a kernel of size (7×7) is applied with a stride of $(2,2)$. The weights of the convolutional layer were once again initialised using He initialisation. An l2 kernel level regulariser with a penalty factor of $1e-5$ is used to regularise each trainable layer. The outputs of the convolutional layer are normalised using batch normalisation before having a ReLU activation function applied. Unless specified, all subsequent convolutional layers follow the $CONV \Rightarrow BATCH\_NORM \Rightarrow RELU$ sequence with the same initialiser and regulariser, although the kernel sizes and strides change per the depth of the layer. The first layer of convolution is followed by a (3×3) max pooling layer with a $(2,2)$ stride. The (3×3) max pooling layer will be the only max pooling layer used throughout the network. The next part of the network consists of stacks of residual layers. All residual modules in ResNet50 use bottlenecking. Three residual modules form the layer named conv2_x by He et al. (He et al., 2015), and are used to learn 256 kernel filter weights. The first two convolution blocks each learn 64 filters, and the bottlenecked convolutional block learns 256 filter values. The layers conv3_x, conv4_x, conv5_x follow a similar pattern, although with differing numbers of residual block repetitions and a differing number of learnable filter values. Finally, average pooling with a pool size (7×7) is used before a dense network of 512 units is trained with a 25% probability of dropout being applied before the final predicted output is generated using a softmax layer. A full description of ResNet50's architecture can be found in (He et al., 2015).

4.4 Xception

The Xception network comprises 36 convolutional layers that form the feature extraction section of the network. Xception contains 22885952 trainable parameters. These convolutional layers are structured into 14 modules, with all modules being connected with a linear residual connection around them, apart from the first and last modules. We used a dense fully-connected layer of 512 units, each having a 25% chance of being dropped out during training for a classification base. The final layer used softmax activation to generate output. Once again, an l2 kernel level regulariser with a penalty factor of $1e-5$ was applied to convolutional layers. A full description of the Xception architecture can be found in (Chollet, 2017).

5 EXPERIMENTAL VALIDATION

5.1 Experimental Data

The largest current example of a mammographic imaging data sets is the Digital Database for Screening Mammography (DDSM). The DDSM was collected in the early 90s and had an image quality far lower than its modern counterparts. Additionally, the data set contains very imbalanced data regarding the number of normal cases to cases containing abnormalities (Heath et al., 1998). Recently researchers commonly use an updated and standardised version of the DDSM, namely the Curated Breast Imaging Subset of DDSM (CBIS-DDSM), for mammographic analysis when using a public data set is required. We decided to use the CBIS-DDSM as this study's data set to directly and accurately compare our results and existing research. We would use the CBIS-DDSM for abnormality classification.

In an effort to address the challenges of using the DDSM, Lee et al. proposed further standardisation to the existing data set (Lee et al., 2017). A subset of the DDSM containing the cancerous and benign studies was updated to remove chain codes and artefacts from the images. Precise ROI segmentation masks were made by a trained radiologist and stored as part of the data set in binary masks of the exact dimensions as its associated study image. The images have also been decompressed and converted from a lossless JPEG format to DICOM format and are readily available through a web service or an easy-to-use desktop application provided by The Cancer Imaging Archive (TCIA). The data set consists of images of both mass and calcification cases, totalling 3568 images in both bilateral craniocaudal (CC) and mediolateral oblique (MLO) views. The original DDSM data set was collated from four medical institutions, with each institution using different digitiser technology (Heath et al., 1998). Each digitiser scanned images at differing sampling rates and grey levels, resulting in inconsistent opacity levels across the data set. As such, the curators of the CBIS-DDSM chose to clip opacity values and remap the grey levels to 16-bit grayscale between decompression and conversion to DICOM. The binary class breakdown of the CBIS-DDSM is **P**ositive cases - 1457 (40.84%), **N**egative cases - 2111 (59.16%).

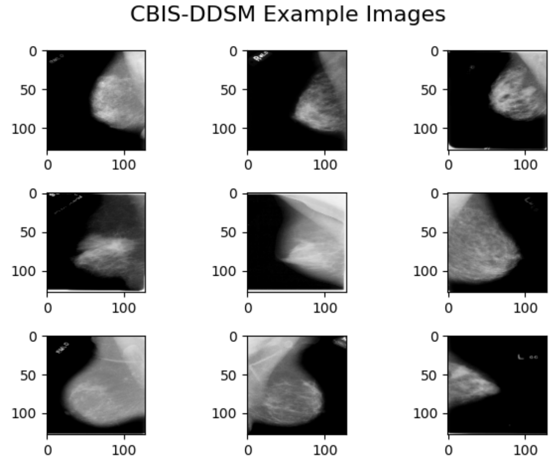

Figure 1: Examples of images found within the CBIS-DDSM data set.

5.2 Configuration Permutations

The collection of results was accomplished by running four unique configurations of models. The various permutations of the experiments we conducted to assess the efficacy of deep learning for medical abnormality classification can be seen in table 1. The experiment Ids are formed using a key explained in the caption of table 1. We used the test-train split stipulated by the authors of (Sawyer-Lee et al., 2016) in the accompanying metadata files from TCIA. The ResNet50 and Xception models and their optimised variants were compared on the abnormality classification.

Table 1: Experimental configurations permutations for the baseline and their respective GA counterparts.

Id	Architecture	Metaheuristic
CRD	ResNet50	-
CRD-GA	ResNet50	GA
CXD	Xception	-
CXD-GA	Xception	GA

5.3 Results

In this study's context, abnormality classification is the process of delineating whether or not a given mammogram image containing an abnormality is malignant or benign. We will use the full-size mammogram images from the CBIS-DDSM data set for this

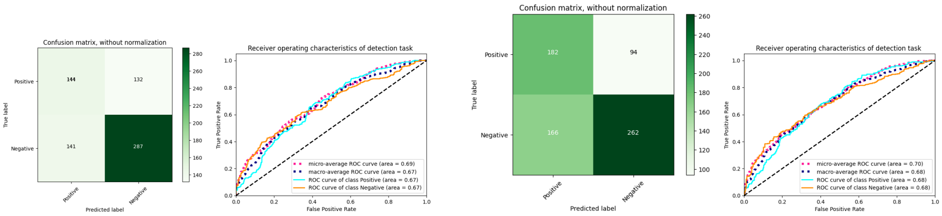

(a) CRD (b) CRD-GA

Figure 2: Comparison of the metrics generated for the abnormality classification task with ResNet50.

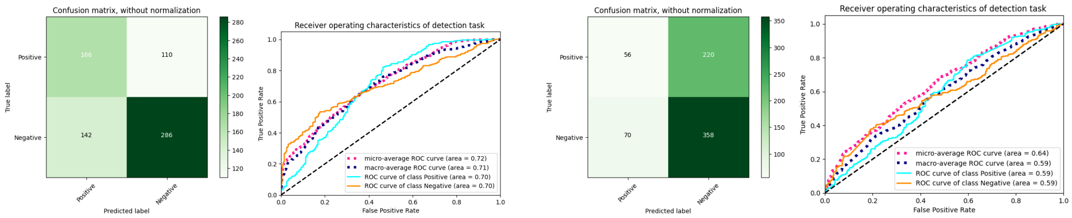

(a) CXD (b) CXD-GA

Figure 3: Comparison of the metrics generated for the abnormality classification task with Xception.

Table 2: Results for the binary classification of abnormalities.

Id	Loss	Accuracy	Precision	Recall
CRD	**0.6364**	63.49	61.91	62.06
CRD-GA	0.6510	**63.92**	**63.92**	**63.92**
CXD	**0.5882**	**64.20**	**63.06**	**63.48**
CXD-GA	0.6928	60.79	60.79	60.79

task, given that it is a curated subset of the DDSM containing only suspicious cases. For metrics generated from training on CBIS-DDSM, a positive case denotes an image containing at least one malignant mass or calcification.

Table 2 shows the results of the control experiments for the binary classification task, where an image from a medical study is presented to a model which assigns a true/false label to the image on whether the image contains a malignant or benign abnormality. The metric plots generated using the control networks can be seen in figures 2 and 3.

Interestingly enough, the genetic algorithm improved the number of true positives identified for ResNet50 when comparing CRD-GA to CRD-I, although the loss score did deteriorate, as can be seen in table 2. Additionally, the fine-tuned ResNet50 models did minimise the false positives found while increasing the number of true positives but altered the false negative rate to do so, likely due to the biases inherent in the objective function, stipulated by equation 1. The fine-tuning led to improved precision but a weakened recall.

6 DISCUSSION

In section 3, we reviewed literature that had applied deep learning methodologies to abnormality classification in mammography. As a reminder, the salient experimental setup details for the works previously discussed are:

1. Tsochatzidis et al. compared an array of networks, including a pre-trained ResNet50, at abnormality classification (Tsochatzidis et al., 2019). Only images containing masses were used. The input images were cropped windows centred around the ROI and were resized to 224 × 224. Data augmentation was applied to the data set.
2. Almeida et al. used a VGGNet16 to perform abnormality classification on the CBIS-DDSM. Images were resized to 224 × 224, and data augmentation was used (Almeida et al., 2021).

An unfortunate restriction placed on our research was the availability of sufficient hardware resources, leading us to run our experiments with an input size of 128 × 128, far lower than the usual 224 - 256 squared pixel inputs seen in the similar work. This constraint increases the challenge of each task, considering that the abnormalities present in full-size mammogram images in the CBIS-DDSM take up a very small area of pixels (Sun et al., 2018). Tsochatzidis et al. cropped into an area centred around the annotated ROIs of mass cases. We feel this is unrepresentative of the real-world tasks of a radiologist. In the case of the classification tasks that used this strategy, we felt this would give the network an unfair advantage as it would quickly learn that the abnormality was centre aligned. Moreover, all the similar works only considered the mass cases of their selected data set when performing their respective tasks. A contribution that this study makes is providing results of various models that consider both calcifications and masses.

The accuracy scores of the control experiments commonly landed in the region of 60%-65%, accompanied by usually poor precision and recall scores. There is a cyclical relationship between the imbalanced data set towards the number of negative samples and the neural networks favouring negative predictions, as seen in the accompanying confusion matrices. A bias toward predicting negative cases generates a large number of false negatives, which in turn decreases the recall/sensitivity of a model.

7 CONCLUSION

This study was undertaken to determine if a genetic algorithm could update a convolutional neural network's internal parameters within the context of abnormality classification in mammographic imaging. We tested the genetic algorithm on ResNet50 and Xception architectures. While minor improvements were made concerning the true positive rate of the fine-tuned ResNet model, the Xception model's metric performance substantially degraded. It is difficult to conclude the effectiveness of using the genetic algorithm presented here for optimising convolutional neural networks. Future work on this topic may consider investigating the effects of evolutionary optimisation on other CNN architectures.

REFERENCES

Almeida, R., Chen, D., Filho, A., and Brandão, W. (2021). Machine learning algorithms for breast cancer detection in mammography images: A comparative study. *Proceedings of the 23rd International Conference on Enterprise Information Systems*.

Chollet, F. (2017). Xception: Deep learning with depthwise separable convolutions.

Crean, M., Rouger, M., and Zizka, D. (2012). Making cancer visible: The role of imaging in oncology.

Dauer, L. (2019). *Dose, benefit, and risk in medical imaging*. Imaging in medical diagnosis and therapy. CRC Press.

Engelbrecht, A. P. (2008). *Computational intelligence: an introduction*. CRC Press.

He, K., Zhang, X., Ren, S., and Sun, J. (2015). Deep Residual Learning for Image Recognition. *arXiv e-prints*, page arXiv:1512.03385.

Heath, M., Bowyer, K., Kopans, D., Kegelmeyer, P., Moore, R., Chang, K., and Munishkumaran, S. (1998). Current status of the digital database for screening mammography. *Computational Imaging and Vision Digital Mammography*, page 457–460.

Holland, J. H. (2010). *Adaptation in natural and artificial systems: an introductory analysis with applications to biology, control, and artificial intelligence*. MIT Press.

Keras (2017). Keras documentation: Resnet and resnetv2.

Kim, E.-K., Kim, H.-E., Han, K., Kang, B. J., Sohn, Y.-M., Woo, O. H., and Lee, C. W. (2018). Applying data-driven imaging biomarker in mammography for breast cancer screening: Preliminary study. *Scientific Reports*, 8(1).

Kooi, T., Litjens, G., Ginneken, B. V., Gubern-Mérida, A., Sánchez, C. I., Mann, R., Heeten, A. D., and Karssemeijer, N. (2017). Large scale deep learning for computer aided detection of mammographic lesions. *Medical Image Analysis*, 35:303–312.

Lee, J.-G., Jun, S., Cho, Y.-W., Lee, H., Kim, G. B., Seo, J. B., and Kim, N. (2017). Deep learning in medical imaging: General overview. *Korean Journal of Radiology*, 18(4):570.

Miller, B. and Goldberg, D. (1995). Genetic algorithms, tournament selection, and the effects of noise. *Complex Systems*, 9:193–212.

Noel, M. M. (2012). A new gradient based particle swarm optimization algorithm for accurate computation of global minimum. *Applied Soft Computing*, 12(1):353–359.

Oldewage, E. T. (2017). *The perils of particle swarm optimization in high dimensional problem spaces*. University of Pretoria.

Pawełczyk, K., Kawulok, M., and Nalepa, J. (2018). Genetically-trained deep neural networks. *Proceedings of the Genetic and Evolutionary Computation Conference Companion*, page 63–64.

Sawyer-Lee, R., Gimenez, F., Hoogi, A., and Rubin, D. (2016). Curated breast imaging subset of ddsm.

Sun, H., Li, C., Liu, B., and Wang, S. (2018). Aunet: Breast mass segmentation of whole mammograms. *CoRR*, abs/1810.10151.

Tabár, L., Vitak, B., Chen, T. H.-H., Yen, A. M.-F., Cohen, A., Tot, T., Chiu, S. Y.-H., Chen, S. L.-S., Fann, J. C.-Y., Rosell, J., and et al. (2011). Swedish two-county trial: Impact of mammographic screening on breast cancer mortality during 3 decades. *Radiology*, 260(3):658–663.

Tsochatzidis, L., Costaridou, L., and Pratikakis, I. (2019). Deep learning for breast cancer diagnosis from mammograms—a comparative study. *Journal of Imaging*, 5:37–48.

Whitley, D., Starkweather, T., and Bogart, C. (1990). Genetic algorithms and neural networks: Optimizing connections and connectivity. *Parallel Computing*, 14(3):347–361.